Mathematical Modeling Predicts How to Accelerate Blood Biomarker-Based Early Cancer Detection

Supplementary Material

Sharon S. Hori and Sanjiv S. Gambhir

Derivation of Model Equations.

Figure 1 shows a basic schematic for the 1-compartment model of biomarker secretion and tumor growth. Here, we derive the equation for the mass of biomarker in plasma, $q_{PL}(t)$, for the mono-exponential and Gompertzian growth models.

1. Mono-Exponential Growth Model

The change in plasma biomarker mass with respect to time is

$$\frac{dq_{PL}(t)}{dt} = u_T(t) + u_H(t) - k_{EL}q_{PL}(t). \quad \text{(Eq. 1)}$$

The rate of entry of biomarker into plasma is the sum of inputs from tumor cells,

$$u_T(t) = f_{PL,T}R_T N_T(t), \quad \text{(Eq. 2)}$$

and from healthy cells,

$$u_H(t) = f_{PL,H}R_H N_H(t) \quad \text{(Eq. 3)}$$

Tumor cell growth is represented by the mono-exponential equation,

$$N_T(t) = N_{T,0}e^{k_{GR}t}, \quad \text{(Eq. 4)}$$

and healthy cell population is assumed constant,

$$N_H(t) = N_{H,0}. \quad \text{(Eq. 5)}$$

Combining Eqs. 1-5 gives

$$\frac{dq_{PL}(t)}{dt} = f_{PL,T}R_T N_{T,0}e^{k_{GR}t} + f_{PL,H}R_H N_{H,0} - k_{EL}q_{PL}(t). \quad \text{(Eq. 6)}$$

Eq. 6 can be solved numerically or analytically for $q_{PL}(t)$. The analytical solution of Eq. 6 can be obtained by taking the Laplace Transform,

$$sQ_{PL}(s) - q_0 = \frac{f_{PL,T}R_T N_{T,0}}{s - k_{GR}} + \frac{f_{PL,H}R_H N_{H,0}}{s} - k_{EL}Q_{PL}(s) \quad \text{(Eq. 7)}$$

Solving for $Q_{PL}(s)$

$$Q_{PL}(s) = \frac{-f_{PL,H}R_H N_{H,0}k_{GR} - \left(k_{GR}q_0 - f_{PL,H}R_H N_{H,0} - f_{PL,T}R_T N_{T,0}\right)s + q_0 s^2}{s\left(s - k_{GR}\right)\left(s + k_{EL}\right)} \quad \text{(Eq. 8)}$$

Taking the inverse Laplace transform of Eq. 8 gives

$$q_{PL}(t) = A + Be^{k_{GR}t} + Ce^{-k_{EL}t} \quad \text{(Eq. 9)}$$

where

$$A = \frac{f_{PL,H}R_H N_{H,0}}{k_{EL}}$$

$$B = \frac{f_{PL,T}R_T N_{T,0}}{\left(k_{EL} + k_{GR}\right)}$$

$$C = q_0 - \frac{f_{PL,T}R_T N_T}{\left(k_{EL} + k_{GR}\right)} - \frac{f_{PL,H}R_H N_{H,0}}{k_{EL}}$$

Eq. 9 is set equal to detectable mass of biomarker in plasma $d \times V_{PL}$ (in the case of biomarker secretion by tumor cells only) or to cut-off limit $c \times V_{PL}$ (in the case of biomarker secretion by tumor and healthy cells), and can subsequently be solved for t to determine the earliest possible detection time t_D.

2. Gompertzian Growth Model

For the Gompertzian model, we replace Eq. 4 with

$$N_T(t) = N_{T,0}e^{\left(\frac{k_{GR}}{k_{DECAY}}\right)\left(1 - e^{-k_{DECAY}t}\right)} \quad \text{(Eq. 10)}$$

Eq. 6 is then solved numerically for $q_{PL}(t)$, and set equal to $d \times V_{PL}$ or $c \times V_{PL}$.

Supplementary Methods

Parameter Ranges Examined

We performed one-way sensitivity analyses on the following 9 parameters, with parameter ranges listed explicitly in Table 2 and justified below.

1. $f_{PL,T}$, the fraction of biomarker entering plasma. Because the fraction of interstitial CA125 entering plasma has not been measured, we used a baseline value of $f_{PL,T} = 0.1$, as has been done previously (*1*), and then examined a range of $f_{PL,T}$ values from 1×10^{-4} to 1.

2. R_T, the biomarker shedding rate from tumor cells. The shedding rates of CA125 in ovarian cancer cell lines OVCAR-3, SK-OV8, SK-OV-3 range from 2 to 13 U/(10^5 cells)/(48 h) (*2*). We used a baseline CA125 shedding rate of $R_T = 4.5\times10^{-5}$ U/cell/day. To account for possibly higher shedding rates due to influences from the tumor microenvironment *in vivo*, as well as varying basal shedding rates between individual patients, we simulated a wide range of shedding rates from 4.5×10^{-11} to 0.45 U/cell/day.

3. $N_{T,0}$, the initial number of biomarker-shedding tumor cells. To simulate the genesis of a tumor, we set $N_{T,0} = 1$, and then examined a range of values up to 1×10^{10} cells, at which point the tumor is assumed to be well-established. Values of $N_{T,0} > 1$ can represent scenarios after the first malignant cell has proliferated, e.g., when the primary tumor is more established, metastases have developed, or the cancer has recurred.

4. k_{GR}, the growth rate of the tumor cell population. Brown and Palmer have estimated that human ovarian carcinomas have a doubling time of 4 months during the early disease stages (Stages I and II), and a 2.5 month doubling time during late disease stages (Stages III and IV) (*3*). Baseline tumor growth rate $k_{GR} = 5.8\times10^{-4}$ day^{-1} was calculated using the formula $k_{GR} = (\ln 2)/(t_{DT})$, where tumor doubling time $t_{DT} = 120$ days. We explored an extreme range of growth rates from 3.5×10^{-4} (200 day doubling time) to 0.58 day^{-1} (1 day doubling time).

5. k_{EL}, the elimination rate of biomarker from plasma. The mean serum half-life for CA125 is 6.3 days (*4*), so we used a baseline elimination rate of $k_{EL} = (\ln 2)/(6.3 \text{ day}) = 0.1104$ day^{-1}. We simulated an extreme range of elimination rates from 1.1×10^{-6} to 5.12 day^{-1}, (corresponding to half-times ranging from 1720 yr to 3.25 hr).

6. k_{decay}, the rate of decay of the growth rate. The values of k_{decay} have not been estimated for human ovarian carcinoma, but a linear correlation between k_{GR} and k_{decay} has been shown for

the human colon carcinoma cell line LoVo (*5*). We used a baseline value of $k_{decay} = 1\times10^{-4}$ and then simulated a range of values from 1.29×10^{-6} to 2.15×10^{-4}.

7. *d*, the minimum concentration of biomarker detectable in plasma (detection limit of assay). Current clinical CA125 ELISA assays are capable of detecting as low as 1.5 U/ml (*2, 6, 7*). Newer technologies are capable of detecting as low as 50 attomolar (5×10^{-17} M) (*8*). We used a baseline value of d = 1.5 U/ml and simulated a range of detection limits from 5×10^{-10} to 15 U/ml.

8. $f_{PL}R_HN_{H,0}$, the (constant) amount of biomarker shed by healthy cells per unit time. Since experimental values for $f_{PL,H}$, R_H, and $N_{H,0}$ are not known separately for CA125, we examined the unknown lumped product of these values ($f_{PL,H}R_HN_{H,0}$). We used $f_{PL}R_HN_{H,0}$ to determine the effect of background healthy cell biomarker shedding on the estimate of tumor size, because the contributions of tumor vs. healthy cell shed biomarker are unknown. The baseline value for $f_{PL,H}R_HN_{H,0}$ was calculated using the steady-state mass of biomarker,

$$q_{SS} = \frac{f_{PL,H}R_HN_{H,0}}{k_{EL}}.$$

Using the baseline value for k_{EL} (0.1104 day^{-1}) and the measured steady-state value q_{SS} = 13.1 ± 6.8 U/ml (*9*), we calculated a baseline $f_{PL,H}R_HN_{H,0}$ value of 4.56×10^3 U/day. We then simulated a range of values from 4.56×10^{-6} to 4.56×10^4 U/day.

9. *c*, the plasma biomarker "cut-off" level for healthy vs. disease states. The mean plasma CA125 concentration in healthy women, as measured using a monoclonal antibody immunoradiometric CA125 assay, is 13.1 ± 6.8 U/ml (*9*). We used 34.11 U/ml as the baseline value for *c*, as calculated previously (*1*). This is reasonable, as CA125 levels less than 35 U/ml are typically considered normal (*9, 10*). We then simulated a range of cutoff values from 13.6 to 135.8 U/ml (from 53% to approximately 100%).

We note that cutoff level *c* is dependent on the mean CA125 levels in healthy women, $q_{SS} = \frac{f_{PL,H}R_HN_{H,0}}{k_{EL}}$. Because *c* is directly proportional to $f_{PL,H}$, R_H and $N_{H,0}$, increasing lumped product $f_{PL,H}R_HN_{H,0}$ by a factor of *n* would also increase *c* by a factor of *n*. Similarly, *c* is inversely proportional to k_{EL}, so changing k_{EL} to $n\times k_{EL}$ would change *c* to *c*/*n*. Therefore, in the sensitivity analyses, when either $f_{PL,H}R_HN_{H,0}$, or k_{EL} were perturbed, *c* was also proportionally altered.

Supplementary discussion of five example early detection strategies evaluated using the 1-compartmental model.

An important result of this study is the identification of the biological processes involved in biomarker shedding that can (or cannot) be exploited to improve blood biomarker detectability. Here, we used the model to evaluate the following five specific strategies in terms of their ability to detect sub-millimeter diameter tumors:

1. Increasing tumor cell biomarker shedding rate, R_T. (As noted previously, the term "shedding" is intended to include any mechanism of biomarker release into the interstitium, e.g., secretion, cell apoptosis.) At baseline, $R_T = 4.5\times10^{-5}$ U/day/cell (Table 2). In the presence or absence of background biomarker shedding, the model indicates that the most effective method is to increase R_T. We found that increasing R_T by a factor of 10^4 above baseline (or alternatively, using a different biomarker with a 10^4-fold higher R_T) allowed detection of tumors less than $(1\ \text{mm})^3$ in the case of tumor and healthy cell shedding, and less than $(0.39\ \text{mm})^3$ in the case of tumor cell shedding only. Tables 3 and 4 and Figures S2B and S3B also illustrate other outcomes resulting from changing R_T. Increased tumor cell shedding rates are now becoming possible with strategies such as the application of low frequency ultrasound to induce biomarker shedding from suspect tumor sites (*11*).

2. Decreasing the biomarker influx, $f_{PL,H}R_H N_{H,0}$, from healthy (non-cancerous) cells. At baseline, $f_{PL,H}R_H N_{H,0} = 4.56\times10^3$ U/day (Table 2). The ideal cancer biomarker would not be shed by healthy cells. Using the baseline parameter values provided in this study, we quantified that decreasing healthy cell biomarker influx 10^4-fold would allow detection of sub-millimeter tumors (Table 2). While it may not be physiologically plausible to halt shedding of a biomarker by healthy cells, this result implies that the ideal candidate biomarker should not be released from healthy cells at an influx rate more than 0.456 U/day. This translates to a 10^4-fold decrease in the mean steady-state biomarker concentration observed in healthy patients (without cancer); thus q_{SS}/V_{PL} should not exceed 0.0013 U/ml. Although we are unaware of any clinical blood biomarker that satisfies this requirement, this provides a more rigorous guideline as to how the biomarker production levels by tumor cells vs. healthy cells could be defined.

3. Decreasing the assay detection limit, d. At baseline, $d = 1.5$ U/ml (Table 2). In the case of shedding by tumor cells only, decreasing d from 1.5 to 1.5×10^{-3} U/ml (a 10^3-fold decrease) would allow detection of tumors as low as 0.85 mm in diameter (Figures S2G and Table 3). This

is becoming possible as newer detection technologies, such as the magneto-nanosensor being developed in our group, are capable of detecting biomarker concentrations as low as 50 attomolar (5×10^{-17} M) (*8*). The model suggests that a 10^6-fold decrease in d would be required to detect tumors smaller than $(0.1\text{ mm})^3$. In the case of background shedding by healthy cells, d is essentially irrelevant because plasma biomarker levels presumably exceed the detection limit.

4. Decreasing biomarker elimination rate from plasma, k_{EL}. At baseline, $k_{EL} = 0.11\text{ day}^{-1}$ (Table 2). For shedding by tumor cells only, if k_{EL} is decreased to 0.5% of its baseline value, then a tumor of volume $(3.21\text{ mm})^3$ could be detected 7.4 years after its genesis (Figure S2F). Decreasing k_{EL} any further would not improve early detection because the detection limit of the assay would become the limiting factor. For shedding by tumor and healthy cells, if k_{EL} is decreased, then c would proportionally increase; thus the minimum detection volume (and corresponding time until detection) would not decrease (Figure S3F). Therefore, using a biomarker that maintains a long half-life in blood is not the most effective solution.

5. Increasing the fraction of biomarker entering plasma, $f_{PL,T}$. At baseline, $f_{PL,T} = 0.1$ (Table 2). Interestingly, even if 100% of shed biomarker were to enter blood, the model indicates that the smallest detectable tumor for a biomarker shed by both tumor and healthy cells would only be $(9.49\text{ mm})^3$ vs. baseline $(20.44\text{ mm})^3$, and would become detectable (with an assay of d = 1.5 U/ml) approximately 9.0 years after the genesis of the tumor (Table 4). For a biomarker shed by tumor cells only, the smallest detectable tumor would be $(3.94\text{ mm})^3$ vs. baseline $(8.48\text{ mm})^3$, becoming detectable 7.7 years after the genesis of the tumor (Table 3). Detecting smaller tumor volumes would not be possible with an assay of this sensitivity because $f_{PL,T}$ cannot be increased beyond 1.

References

1. A. M. Lutz, J. K. Willmann, F. V. Cochran, P. Ray, S. S. Gambhir, Cancer screening: a mathematical model relating secreted blood biomarker levels to tumor sizes. *PLoS Med.* **5**, e170 (2008).
2. A. G. Zeimet, C. Marth, F. A. Offner, P. Obrist, M. Uhl-Steidl, H. Feichtinger, S. Stadlmann, G. Daxenbichler, O. Dapunt, Human peritoneal mesothelial cells are more potent than ovarian cancer cells in producing tumor marker CA-125. *Gynecol Oncol.* **62**, 384-389 (1996).
3. P. O. Brown, C. Palmer, The preclinical natural history of serous ovarian cancer: defining the target for early detection. *PLoS Med.* **6**, e1000114 (2009).

4. W. Mastropaolo, Z. Fernandez, E. L. Miller, Pronounced increases in the concentration of an ovarian tumor marker, CA-125, in serum of a healthy subject during menstruation. *Clin Chem.* **32**, 2110-2111 (1986).
5. R. Demicheli, R. Foroni, A. Ingrosso, G. Pratesi, C. Soranzo, M. Tortoreto, An exponential-Gompertzian description of LoVo cell tumor growth from in vivo and in vitro data. *Cancer Res.* **49**, 6543-6546 (1989).
6. S. K. Mongia, M. L. Rawlins, W. E. Owen, W. L. Roberts, Performance characteristics of seven automated CA 125 assays. *Am J Clin Pathol.* **125**, 921-927 (2006).
7. D. Sok, L. J. Clarizia, L. R. Farris, M. J. McDonald, Novel fluoroimmunoassay for ovarian cancer biomarker CA-125. *Anal Bioanal Chem.* **393**, 1521-1523 (2009).
8. R. S. Gaster, D. A. Hall, C. H. Nielsen, S. J. Osterfeld, H. Yu, K. E. Mach, R. J. Wilson, B. Murmann, J. C. Liao, S. S. Gambhir, S. X. Wang, Matrix-insensitive protein assays push the limits of biosensors in medicine. *Nat Med.* **15**, 1327-1332 (2009).
9. P. Kenemans, G. J. van Kamp, P. Oehr, R. A. Verstraeten, Heterologous double-determinant immunoradiometric assay CA 125 II: reliable second-generation immunoassay for determining CA 125 in serum. *Clin Chem.* **39**, 2509-2513 (1993).
10. R. C. Bast, Jr., T. L. Klug, E. St John, E. Jenison, J. M. Niloff, H. Lazarus, R. S. Berkowitz, T. Leavitt, C. T. Griffiths, L. Parker, V. R. Zurawski, Jr., R. C. Knapp, A radioimmunoassay using a monoclonal antibody to monitor the course of epithelial ovarian cancer. *N Engl J Med.* **309**, 883-887 (1983).
11. A. L. D'Souza, J. R. Tseng, K. B. Pauly, S. Guccione, J. Rosenberg, S. S. Gambhir, G. M. Glazer, A strategy for blood biomarker amplification and localization using ultrasound. *Proc Natl Acad Sci U S A.* **106**, 17152-17157 (2009).

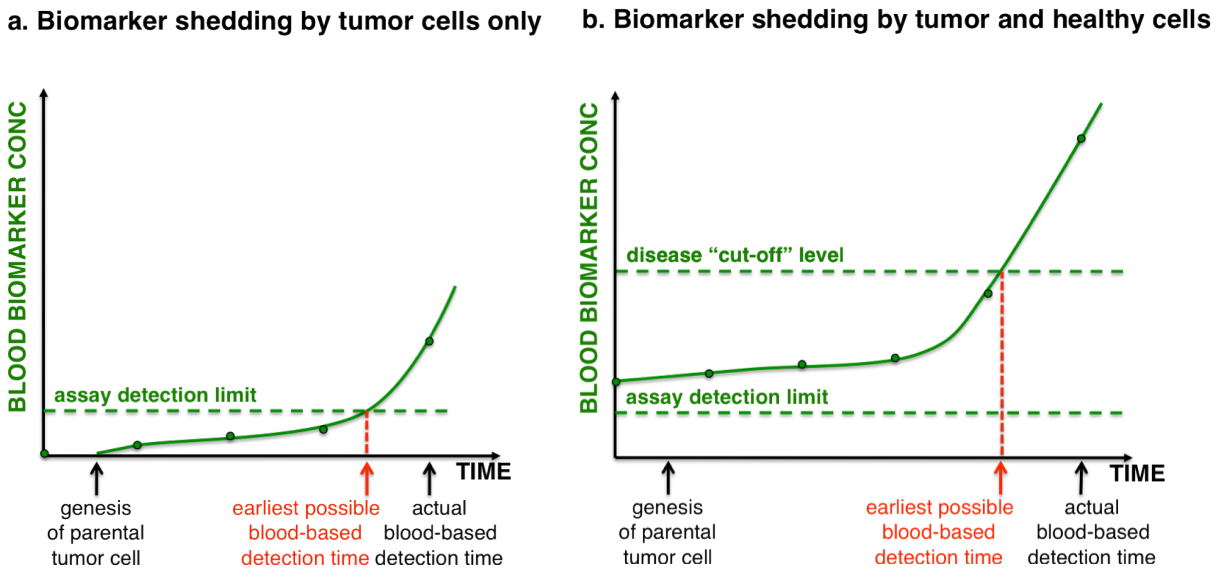

Figure S1. Earliest possible detection time vs. actual blood-based detection times. (A) When biomarker is shed by tumor cells only, the assay detection limit determines the earliest possible blood-based detection time. Green circles represent blood biomarker levels at periodic sampling times. Before the genesis of the parental tumor cell, blood biomarker levels are 0. The actual blood-based detection time occurs when the first blood sampling test exceeds the assay detection limit. (B) When biomarker is also shed by healthy cells, blood biomarker concentrations are presumably already above the assay detection limit. The earliest possible detection time is then determined by the "cut-off" level for healthy vs. disease states. The actual blood-based detection time occurs when the first blood sampling result exceeds the disease "cut-off" level.

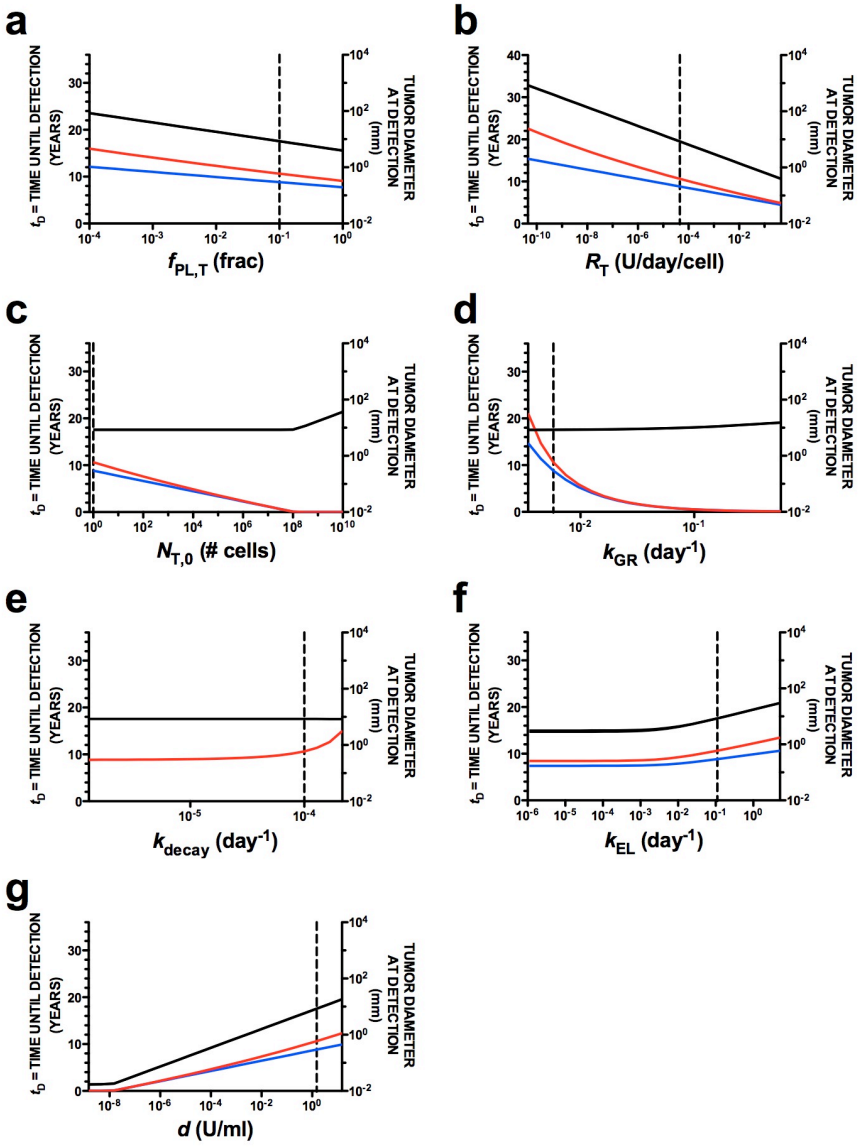

Figure S2. Earliest possible detection time t_D (left y-axis) and diameter of tumor at detection (right y-axis), calculated for the indicated range of parameter values (x-axis) assuming biomarker shedding by tumor cells only. Early detection time t_D was approximated using both mono-exponential (——) and Gompertzian (——) tumor growth models. Tumor diameter (——) was approximated assuming a cell density of 10^6 cells/mm^3. Dashed vertical line (– – –) indicates baseline parameter value. (A) $f_{PL,T}$, the fraction of biomarker entering tumor vasculature. (B) R_T, the biomarker shedding rate per tumor cell. (C) $N_{T,0}$, the initial number of biomarker-shedding tumor cells. (D) k_{GR}, the growth rate of the tumor cell population. (E) k_{decay}, the rate at which the tumor growth rate decreases. (F) k_{EL}, the elimination rate of biomarker from plasma. (G) d, the detection limit of the assay.

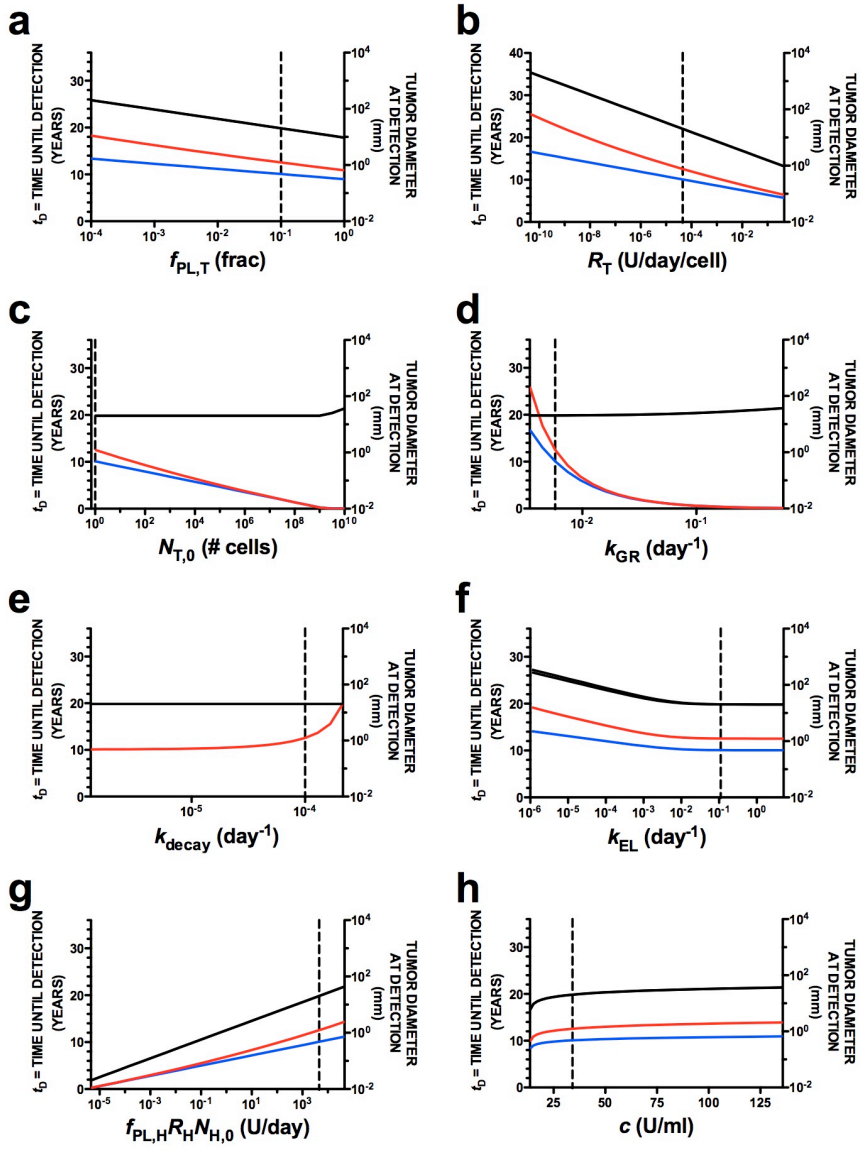

Figure S3. Earliest possible detection time t_D (left y-axis) and diameter of tumor at detection (right y-axis), calculated for the indicated range of parameter values (x-axis) assuming biomarker shedding by tumor and healthy cells. Early detection time t_D was approximated using both mono-exponential (——) and Gompertzian (——) tumor growth models. Tumor diameter (——) was approximated assuming a cell density of 10^6 cells/mm^3. Dashed vertical line (– – –) indicates baseline parameter value. (A) $f_{PL,T}$, the fraction of biomarker entering tumor vasculature. (B) R_T, the biomarker shedding rate per tumor cell. (C) $N_{T,0}$, the initial number of biomarker-shedding tumor cells. (D) k_{GR}, the growth rate of the tumor cell population. (E) k_{decay}, the rate at which the tumor growth rate decreases. (F) k_{EL}, the elimination rate of biomarker from plasma. (G) $f_{PL,H}R_HN_{H,0}$, the biomarker shedding rate for healthy cells. (H) c, the plasma biomarker "cut-off" for healthy and disease states.